

## Electronic Supplementary Information

### Mg-substituted Prussian blue as low-strain cathode material for aqueous Fe-ion batteries

#### Experimental section

##### Materials synthesis

A facile co-precipitation method was performed to prepare MgFeHCF nanocubes. In brief, 2.5 mmol FeSO<sub>4</sub> and 2.5 mmol MgSO<sub>4</sub> were dissolved in 100 ml de-ionized (DI) water to form solution A, while 2.5 mmol K<sub>4</sub>Fe(CN)<sub>6</sub> was dissolved in 100 ml DI water to form solution B. This reaction was carried out by adding solution A into solution B drop by drop for 10 minutes with constant stirring at 60°C. Subsequently, after stirring for 4 hours, the product was washed thoroughly by centrifugation with DI water several times and then allowed to dry in an oven at 70°C overnight. The original FeHCF was synthesized similarly without MgSO<sub>4</sub>.

##### Material characterizations

Scanning electron microscope (SEM)/Transmission electron microscope (TEM) (HRTEM and Energy dispersive spectrometer) were performed with JEOL JSM-7100F scanning electron microscope and JEM-2100F/Titan G2 60-300 transmission electron microscope. X-ray diffraction patterns were recorded by using a D2 discover X-ray diffractometer with Cu K $\alpha$  radiation ( $\lambda = 1.054056 \text{ \AA}$ ), in a  $2\theta$  angular range of 10°-70°. For *in situ* XRD measurements, the battery system was assembled by a mold where the electrode was covered by an X-ray-transparent polyethylene film. The *in situ* XRD signals were acquired by the planar detector in a still mode during the discharge-charge process, and patterns were collected every 2 min (using D8 discover X-ray diffractometer). Raman spectra were collected by a Renishaw INVIA micro-Raman spectroscopy system. Fourier Transform infrared spectroscopy (FT-IR) was measured using a 60-SXB IR spectrometer. X-ray photoelectron spectroscopy (XPS) tests were carried out by the VG Multi Lab 2000. The element contents were

determined by ICP-OES (JY/T015-1996).

### Electrochemical characterizations

The CR2016 coin cells were assembled with the commercial iron foil anode, 0.5 M FeSO<sub>4</sub> aqueous electrolyte, and MgFeHCF cathode. Glass fibre separator (GF/A, Whatman) was used. To manufacture the cathode electrodes, a slurry was mixed at a weight ratio of 70% active materials, 20% acetylene black, and 10% PVDF in NMP solvent and was cast on a graphite paper and dried at 80°C overnight. The mass loading of active materials was about 2 mg cm<sup>-2</sup>. Cell cycling was performed using a battery tester (NEWARE, Shenzhen, China). Cyclic Voltammetry (CV) tests were conducted on EC-LAB. Electrochemical Impedance Spectroscopy (EIS) tests were conducted from 0.01 Hz to 10 MHz with an amplitude of 10mV via Autolab PGSTAT302N. The Fe<sup>2+</sup> diffusion coefficients ( $D_{Fe^{2+}}$ ) was calculated by the simplified equations:

$$D = \frac{R^2 T^2}{2A^2 n^4 F^4 C^2 \sigma^2} \quad \text{Eq. 1.}$$

$$Z_{re} = R_e + R_{ct} + \sigma \omega^{1/2} \quad \text{Eq. 2.}$$

Where R is the gas constant, T is the absolute temperature, A is the surface area of the electrode, n is the number of transferred electrons per molecule upon cycling, F is the Faraday constant, C is the concentration of Fe ion, and  $\sigma$  is the Warburg coefficient. A Land battery test system was applied to perform Galvanostatic Intermittent Titration Technique (GITT) testing at a current density of 50 mA g<sup>-1</sup> from 0.2 to 1.2 V. The  $D_{Fe^{2+}}$  can be calculated by the following equation:

$$D = \frac{4}{\pi \tau} \left( \frac{m_B V_m}{M_B S} \right)^2 \left( \frac{\Delta E_S}{\Delta E_\tau} \right)^2 \left( \tau \ll \frac{L^2}{D_{Fe^{2+}}} \right) \quad \text{Eq. 3.}$$

Where  $m_B$ ,  $V_m$ , and  $M_B$  represent the active mass, the molar volume, and the molar mass of the MgFeHCF material, respectively.  $\tau$  signifies the duration of a current pulse, and  $S$  is the geometric surface of the MgFeHCF electrode.  $\Delta E_S$  represents the voltage gap between the two steady-state voltages in a single-step GITT process, and

$\Delta E_\tau$  is the voltage variation during a current pulse (Fig. S3a and b). All the tests were performed at room temperature.

### **Computational details**

All calculations in this study were performed with the Vienna ab initio Simulation Package (VASP)<sup>1</sup> within the frame of density functional theory (DFT). The exchange-correlation interactions of electron were described via the generalized gradient approximation (GGA) with PBE functional,<sup>2</sup> and the projector augmented wave (PAW) method<sup>3</sup> was used to describe the interactions of electron and ion. Additionally, the DFT-D3 method<sup>4, 5</sup> was used to account for the long-range van der Waals forces present within the system. The Monkhorst-Pack scheme<sup>6</sup> with a 2 x 2 x 2 k-point mesh was used for the integration in the irreducible Brillouin zone. The kinetic energy cut-off of 460 eV was chosen for the plane wave expansion. The lattice parameters and ionic position were fully relaxed, and the total energy was converged within 10<sup>-5</sup> eV per formula unit. The final forces on all ions are less than 0.02/Å.

**Table S1.** Structure parameters of MgFeHCF.

		x	y	z	Occ.	U	Site	Sym.
1 Fe	Fe3	0	0	0.5	0.826	0.062	4b	m-3m
2 Fe	Fe2	0	0	0	1	0.07	4a	m-3m
3 C	C1	0	0	0.175	1	0.059	24e	4m.m
4 N	N1	0	0	0.286	1	0.067	24e	4m.m
5 K	K1	0.25	0.25	0.25	0.553	0.236	8c	-43m
6 Mg	Mg1	0	0	0.5	0.174	0.062	4b	m-3m

**Table S2.** ICP and elemental analysis results of MgFeHCF and FeHCF.

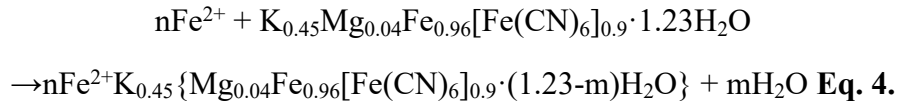
	K content	Fe content	C content	N content	Mg content
MgFeHCF	0.24	0.96	2.9	2.91	0.04
FeHCF	0.08	1	2.59	2.67	

**Table S3.** Compositions of the MgFeHCF and FeHCF and Theoretical Capacity

sample	formula	theoretical capacity (mAh g <sup>-1</sup> )
MgFeHCF	K <sub>0.45</sub> Mg <sub>0.04</sub> Fe <sub>0.96</sub> [Fe(CN) <sub>6</sub> ] <sub>0.9</sub> ·1.23H <sub>2</sub> O	94
FeHCF	K <sub>0.14</sub> Fe[Fe(CN) <sub>6</sub> ] <sub>0.81</sub> ·1.89H <sub>2</sub> O	100.3

Meanwhile, the possible electrochemical reaction formula can be expressed as:

For the MgFeHCF:



For the FeHCF:

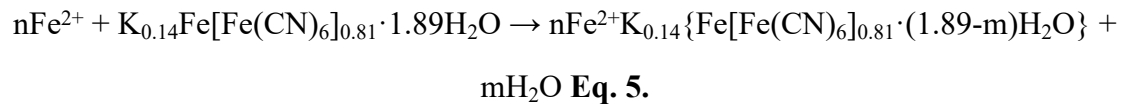


**Table S4.** Comparison of volume changes of several materials.

Cathode	Volume Change	System
HW-PB <sup>7</sup>	5.54%	SIBs
$\text{K}_{0.220}\text{Fe}[\text{Fe}(\text{CN})_6]_{0.805} \cdot 4.01\text{H}_2\text{O}$ <sup>8</sup>	4.96%	KIBs
Fe-PBA <sup>9</sup>	2.47%	LIBs
$\text{Li}_{1.2}\text{Ni}_{0.4}\text{Ru}_{0.4}\text{O}_2$ <sup>10</sup>	2.63%	LIBs
ZnHCF <sup>11</sup>	3%	K/ZIBs
LiFePO <sub>4</sub> <sup>12</sup>	6.8%	LIBs
Co-NVO <sup>13</sup>	0.6%	AZIBs

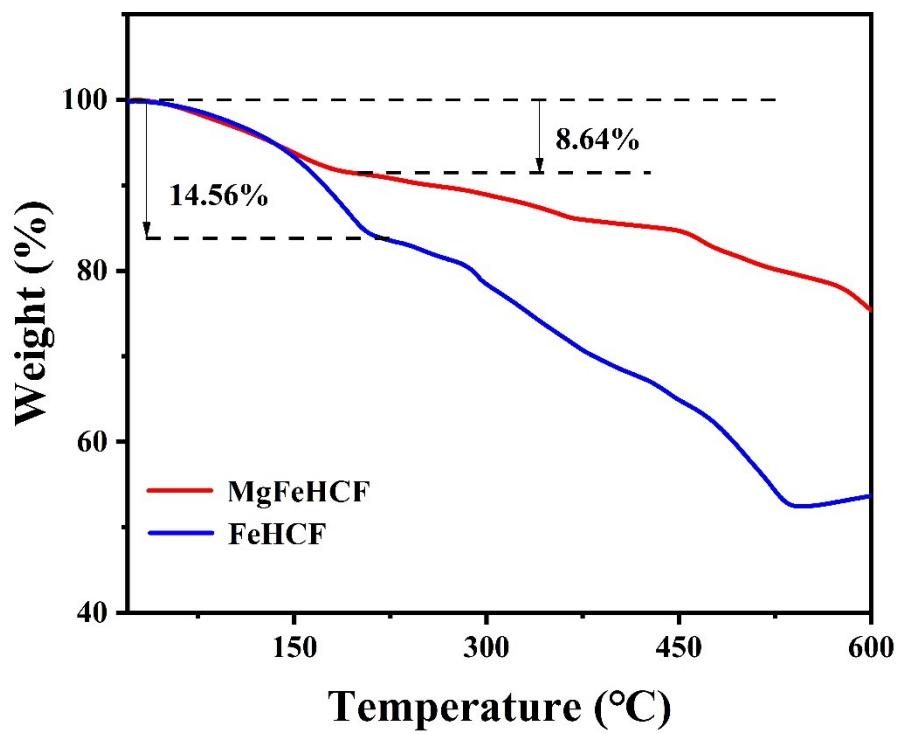
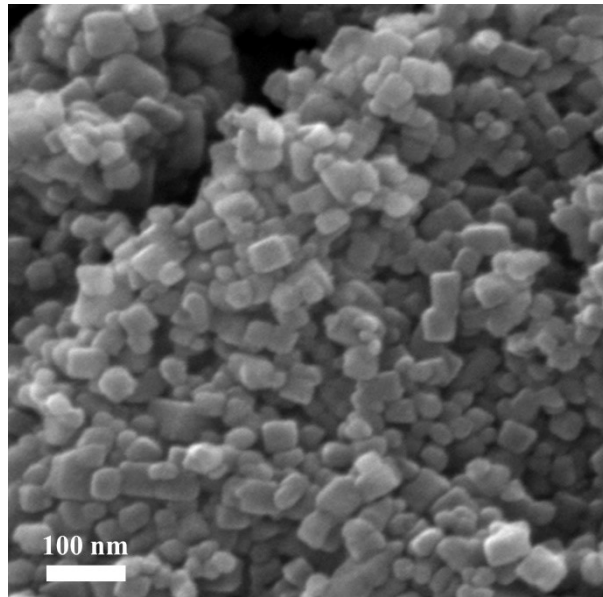
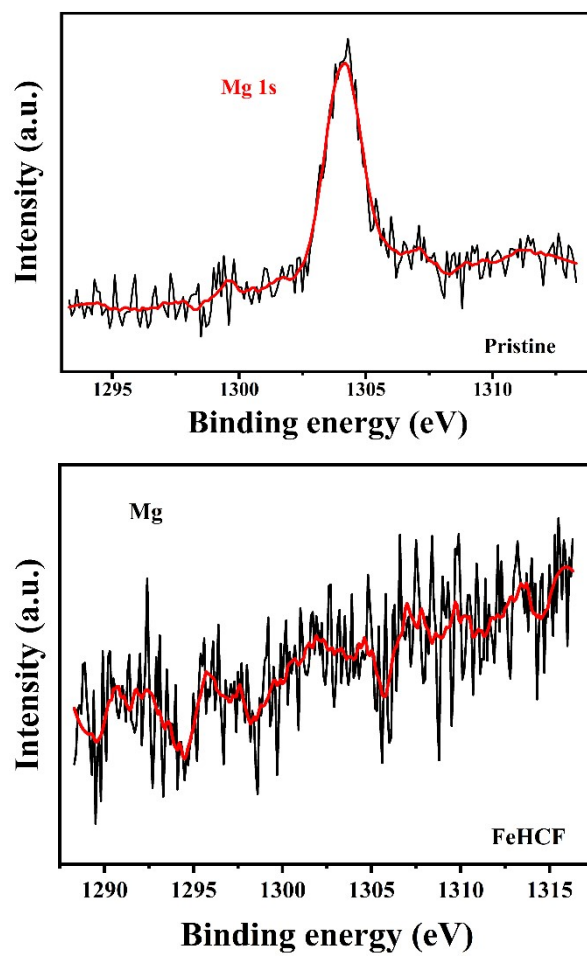


Fig. S1 TGA curves of MgFeHCF and FeHCF.



**Fig. S2** SEM image of FeHCF.



**Fig. S3** Mg 1s XPS spectra of MgFeHCF and FeHCF.

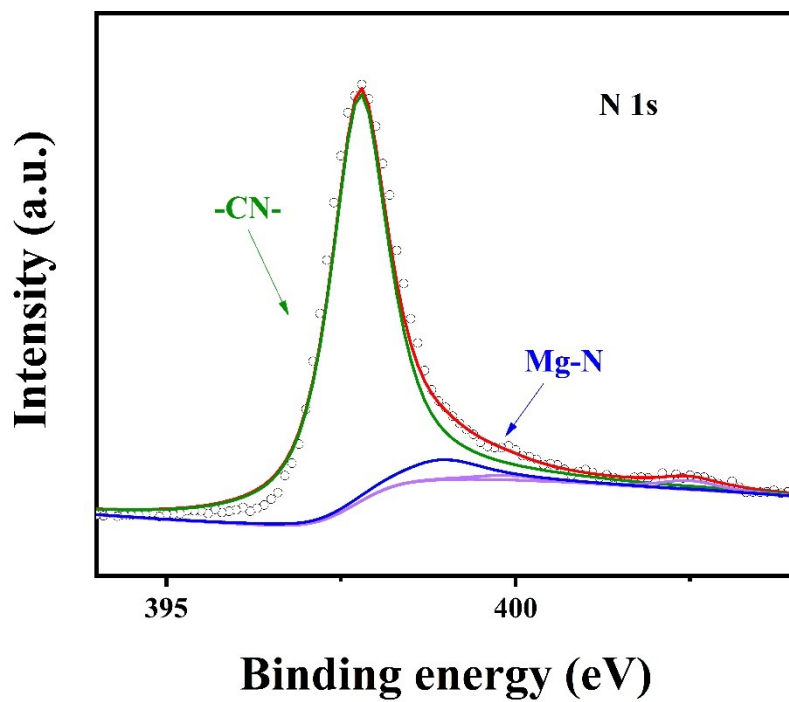


**Fig. S4** N 1s XPS spectra of MgFeHCF.

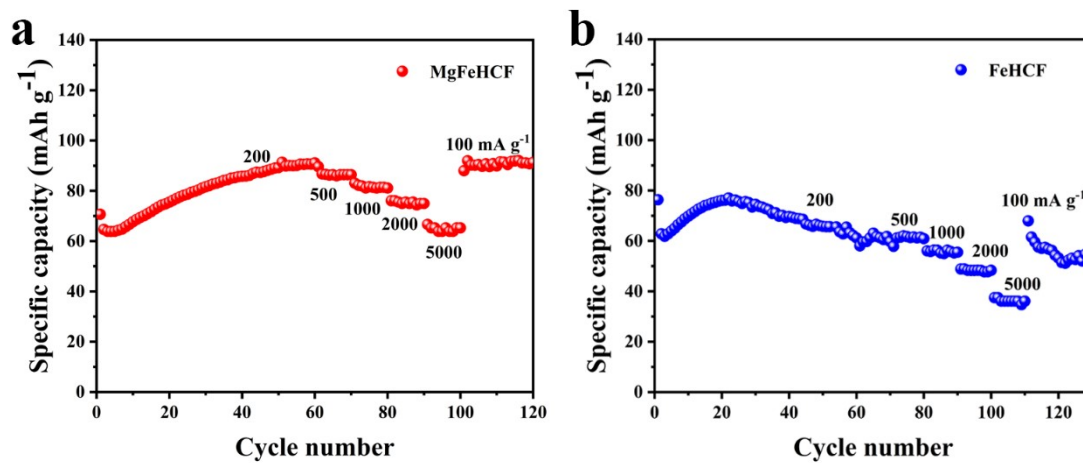


**Fig. S5** The activation process and rate performance of (a) MgFeHCF and (b) FeHCF.

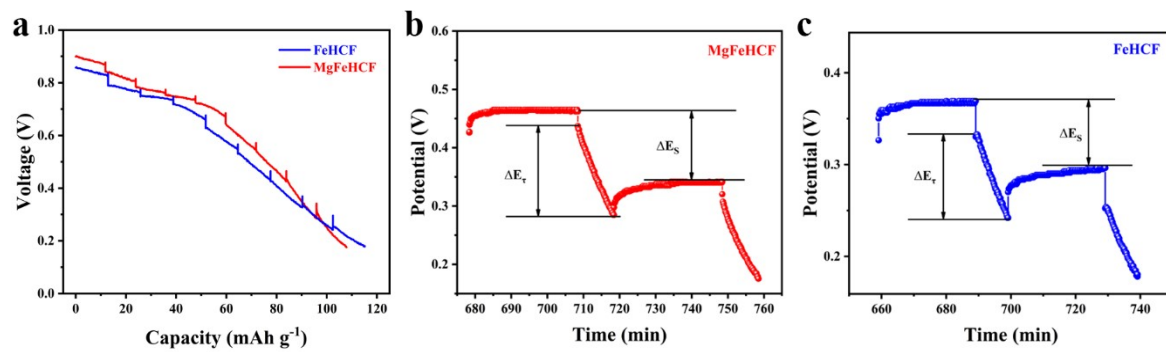


**Fig. S6** (a) GITT curves of MgFeHCF and FeHCF.  $E$  vs.  $\tau$  curves for a single step in GITT experiments of (b) MgFeHCF and (c) FeHCF.

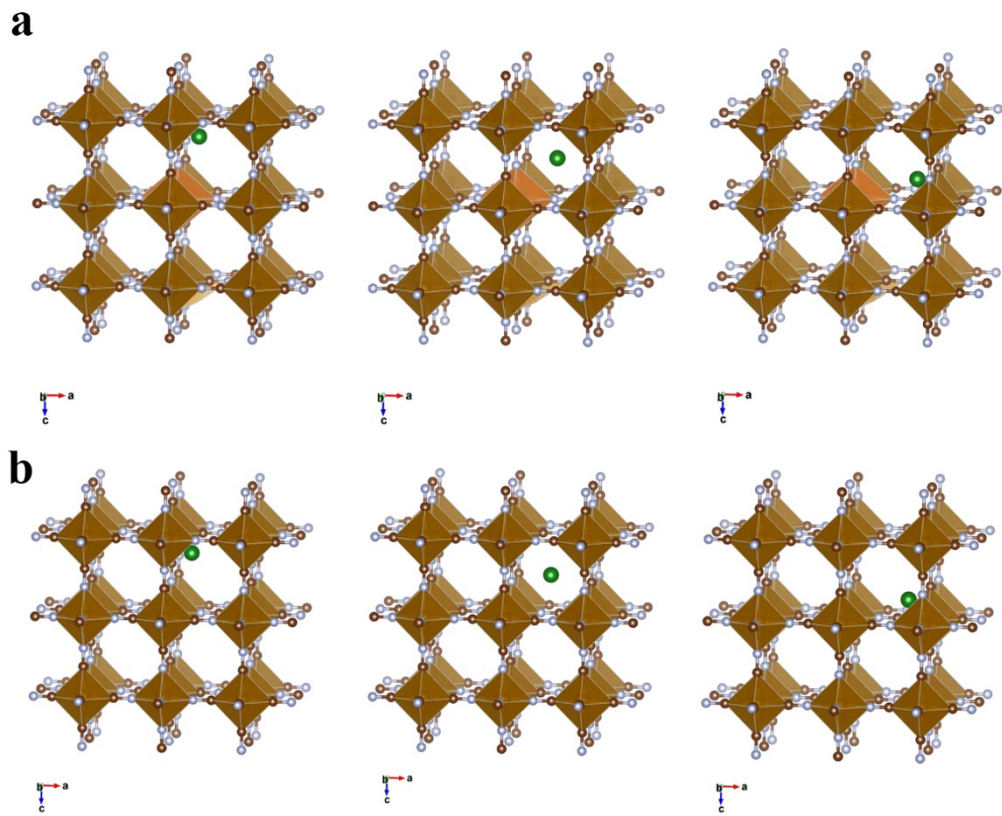


**Fig. S7** The transition state of an iron-ion diffusion within the lattice of the (a) MgFeHCF and (b) FeHCF model structure.

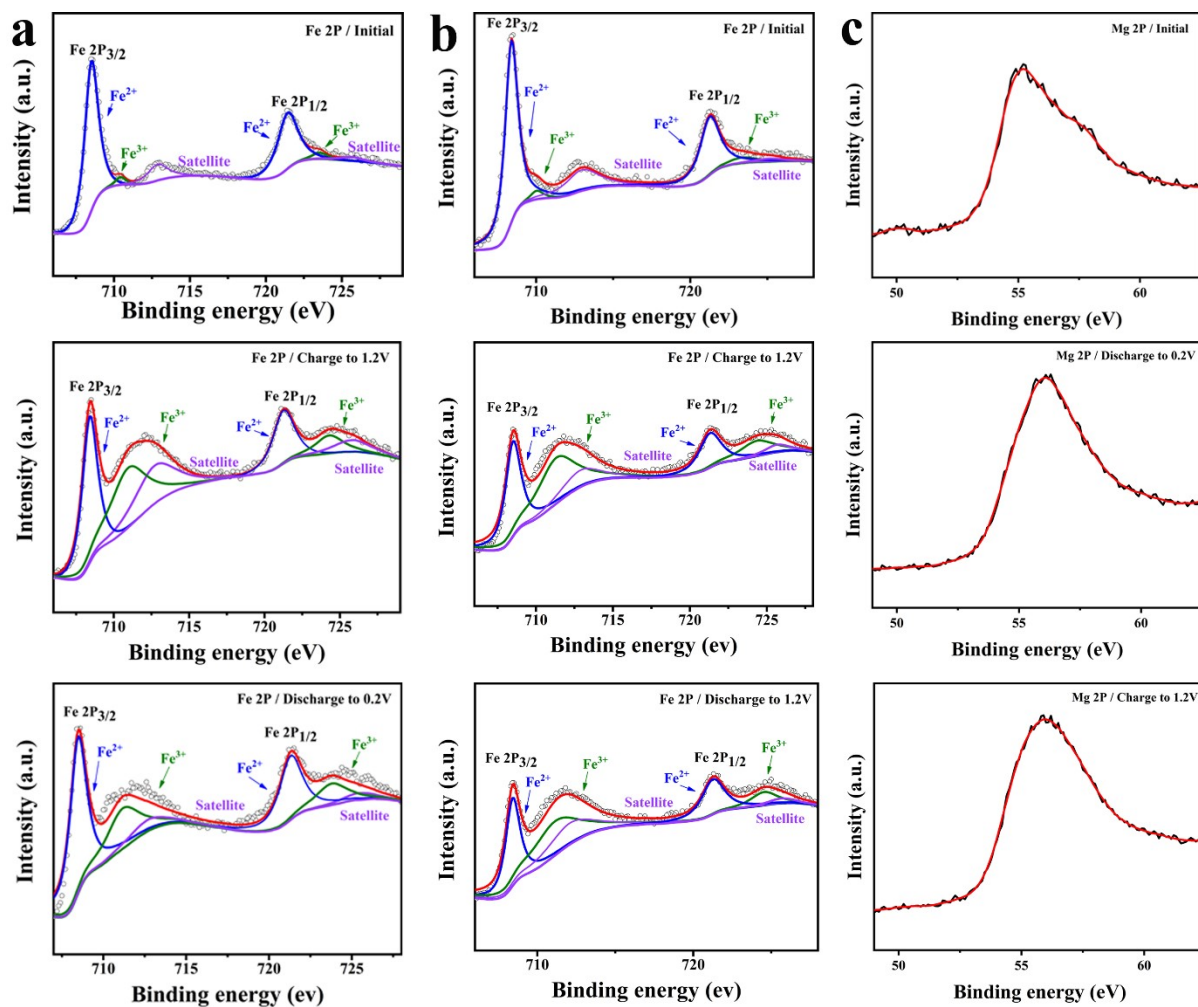
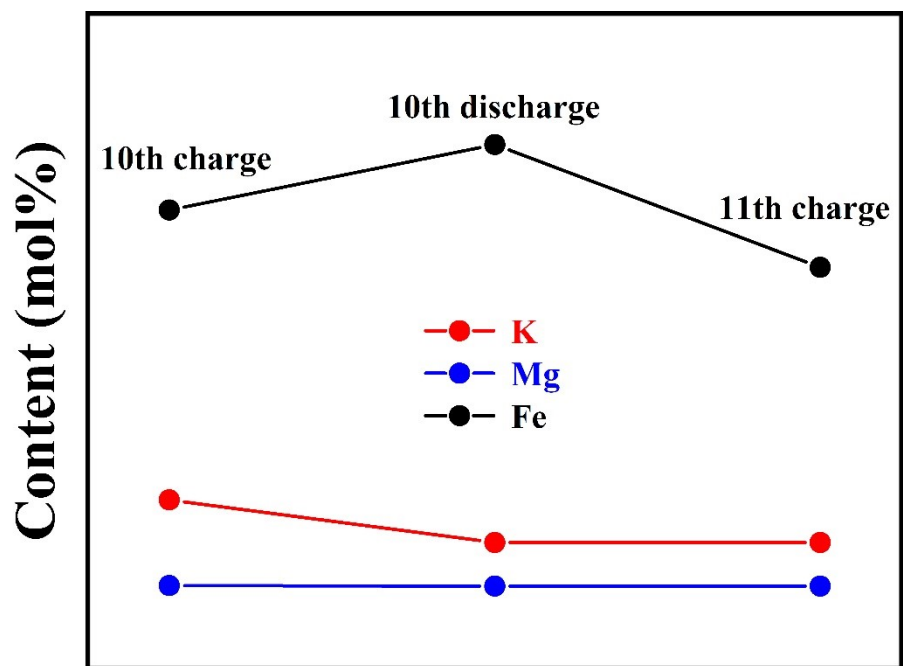


Fig. S8 XPS spectra of Fe 2p (a) MgFeHCF, (b) FeHCF and Mg 2p in (c) MgFeHCF.



**Fig. S9** Content changes of K, Fe and Mg of MgFeHCF during charge and discharge process.

## Supplementary references

1. G. Kresse, J. Furthmuller, *Phys. Rev. B.* **1996**, 54, 11169-11186.
2. J. P. Perdew, K. Burke, M. Ernzerhof, *Phys. Rev. Lett.* **1996**, 77, 3865–3868.
3. G. Kresse; J. Joubert, *Phys. Rev. B.* **1999**, 59, 1758-1775.
4. S. Grimme, J. Antony, S. Ehrlich, H. Krieg, *J. Chem. Phys.* **2010**, 132.
5. S. Grimme, S. Ehrlich, L. Goerigk, *J Comput Chem* **2011**, 32, 1456-1465.
6. H. J. Monkhorst, J. D. Pack, *Phys. Rev. B.* **1976**, 13, 5188-5192.
7. J. Hu, H. Tao, M. Chen, Z. Zhang, S. Cao, Y. Shen, K. Jiang, M. Zhou, *ACS Appl. Mater. Interfaces* **2022**, 14, 12234-12242.
8. C. Zhang, Y. Xu, M. Zhou, L. Liang, H. Dong, M. Wu, Y. Yang, Y. Lei, *Adv. Funct. Mater.* **2017**, 27.
9. J.-H. Lee, J.-G. Bae, H. J. Lee, J. H. Lee, *J. Energy Chem.* **2022**, 70, 121-128.
10. N. Li, M. Sun, W. H. Kan, Z. Zhuo, S. Hwang, S. E. Renfrew, M. Avdeev, A. Huq, B. D. McCloskey, D. Su, W. Yang, W. Tong, *Nat. Commun.* **2021**, 12, 2348.
11. Q. Li, K. Ma, C. Hong, Z. Yang, C. Qi, G. Yang, C. Wang, *Energy Storage Mater.* **2021**, 42, 715-722.
12. C. Delmas, M. Maccario, L. Croguennec, F. Le Cras, F. Weill, *Nat. Mater.* **2008**, 7, 665-671.
13. M. Du, Z. Miao, H. Li, F. Zhang, Y. Sang, L. Wei, H. Liu, S. Wang, *Nano Energy* **2021**, 89.